Detection of peri-implant bone defects using cone-beam computed tomography and digital periapical radiography with parallel and oblique projection

Bardia Vadiati Saberi [1], Negar Khosravifard [2,*], Farnaz Ghandari [3], Arash Hadinezhad [3]

[1]*Dental Sciences Research Center, Department of Periodontics, School of Dentistry, Guilan University of Medical Sciences, Rasht, Iran*
[2]*Dental Sciences Research Center, Department of Maxillofacial Radiology, School of Dentistry, Guilan University of Medical Sciences, Rasht, Iran*
[3]*Department of Maxillofacial Radiology, School of Dentistry, Guilan University of Medical Sciences, Rasht, Iran*

ABSTRACT

Purpose: To compare the diagnostic accuracy of cone-beam computed tomography (CBCT) with that of parallel (PPA) and oblique projected periapical (OPA) radiography for the detection of different types of peri-implant bone defects.
Materials and Methods: Forty implants inserted into bovine rib blocks were used. Thirty had standardized bone defects (10 each of angular, fenestration, and dehiscence defects), and 10 were defect-free controls. CBCT, PPA, and OPA images of the samples were acquired. The images were evaluated twice by each of 2 blinded observers regarding the presence or absence and the type of the defects. The area under the receiver operating characteristic curve (AUC), sensitivity, and specificity were determined for each radiographic technique. The 3 modalities were compared using the Fisher exact and chi-square tests, with $P < 0.05$ considered as statistical significance.
Results: High inter-examiner reliability was observed for the 3 techniques. Angular defects were detected with high sensitivity and specificity by all 3 modalities. CBCT and OPA showed similar AUC and sensitivity in the detection of fenestration defects. In the identification of dehiscence defects, CBCT showed the highest sensitivity, followed by OPA and PPA, respectively. CBCT and OPA had a significantly greater ability than PPA to detect fenestration and dehiscence defects ($P < 0.05$).
Conclusion: The application of OPA radiography in addition to routine PPA imaging as a radiographic follow-up method for dental implantation greatly enhances the visualization of fenestration and dehiscence defects. CBCT properly depicted all defect types studied, but it involves a relatively high dose of radiation and cost. **(*Imaging Sci Dent 2019; 49: 265-72*)**

KEY WORDS: Cone-Beam Computed Tomography; Radiography, Dental, Digital; Peri-Implantitis

Introduction

Long-term monitoring of the condition of the peri-implant soft and hard tissues is a crucial part of evaluating the outcomes of dental implant treatment. The absence of pain, mobility, and infection is generally considered to indicate a desirable treatment outcome. Additionally, precise evaluation of the implant-supporting bone is of utmost importance.[1] Clinically, the early detection of bone loss and osse-

ous defects is essential for assessing the bone architecture and planning regenerative procedures, if necessary. Furthermore, timely detection of bone defects around dental implants could prevent further loss of the bony anchorage, which could eventually result in implant loss if undetected.[2]

The importance of radiographs in depicting the condition of the bone around implants is undisputed. In this regard, special attention has been directed towards the postoperative radiographic evaluation of dental implants, and different radiographic modalities have been used for this purpose, each with its own advantages and disadvantages.[3-5] Among 2-dimensional methods, parallel periapical (PPA) radiography is the most widely used. These radiographs are

acquired with the image receptor placed parallel to the object and the central beam projected perpendicularly to both the image receptor and the object. The resulting images have excellent spatial resolution; however, they are unable to show the condition of bone around the non-proximal areas of implants. This shortcoming can be problematic in some cases, as initial bone loss usually takes place at the bucco-lingual aspect of an implant due to the relative lack of bone thickness in this area.[6]

Three-dimensional (3D) imaging, in contrast, has the benefit of providing volumetric information with accurate and reliable detail at the expense of administering a higher dose of radiation.[7] Currently, cone-beam computed tomography (CBCT) is the technique of choice for various 3D imaging purposes in dentistry.[8] However, in cases in which high-density, metallic objects, such as titanium implants, are positioned within the field of view (FOV), image quality is degraded as a result of streaking and beam-hardening artifacts, rendering the bone around the implant difficult to evaluate.[9] The severity of these artifacts, which in some cases can be sufficient to mask peri-implant bone defects, depends on several factors, including the type of CBCT device used, the FOV dimensions, the position of the object within the FOV, and the application of metal artifact reduction algorithms.[10,11]

In the present study, the efficiency of 3 radiographic techniques including CBCT, PPA radiography, and oblique projected periapical (OPA) radiography for the detection of bone defects around dental implants was assessed. OPA radiography refers to a type of periapical radiography in which, in contrast to PPA radiography, the incident beam is projected at an acute horizontal angle to the object and the image receptor.[12] This study was intended to determine whether OPA radiographs facilitate the detection of peri-implant defects and to compare the results with those obtained through the use of CBCT and PPA radiography.

Materials and Methods

This study was approved by the research ethics committee of Guilan University of Medical Sciences (Approval ID: IR.GUMS.REC.1397.259). Fresh bovine ribs were used to simulate the alveolar bone for implant insertion and defect preparation.[13]

Preparation of the bone samples

Forty blocks of fresh bovine rib with similar dimensions were selected and debrided of the overlying soft tissue. A piece of plastic foam was prepared to fit the bone blocks

in order to keep the samples in a fixed position during the radiographic procedures. Prior to the examinations, digital PPA radiographs were taken from all of the bone blocks to ensure proper bone quality and to exclude bone blocks that already had defects that could interfere with the diagnostic tasks. Subsequently, an osteotomy measuring 4.2×11.5 mm was prepared in each bone block using a Dyna Helix ST implant osteotomy kit (Dyna Dental, Halsteren, The Netherlands).

Creation of the bone defects

The samples were randomly divided into 4 groups. The bone defects to be prepared included fenestrations ($n = 10$), dehiscences ($n = 10$), and either 2- or 3-wall angular defects ($n = 10$). A fourth group consisted of 10 defect-free samples, to be treated as the control group.

A periodontist used a diamond bur to create the defects. Fenestrations were created as rectangular windows on the buccal-resembling sides, 10 mm apically from the edges of the bone blocks (Fig. 1A). Dehiscences were also prepared on the buccal sides of the bone samples, extending downwards from the crestal edge to a point 3 mm apically (Fig. 1B). Angular defects were created as either 3- or 2-wall defects by removing the bone proximal to the osteotomies in 1 or 2 aspects, respectively (Figs. 1C and D). During preparation of each defect, care was taken not to exceed 3 mm along any dimension. This was accomplished through monitoring the defect size by means of a digital caliper (SC-6, Mitutoyo Corporation, Kawasaki, Japan). Following preparation of the defects, 40 implants measuring 4.2×11.5 mm (Dyna Helix, Dyna Dental, Halsteren, The Netherlands) were inserted into the osteotomies. Each bone block was coated with 1.5 cm of wax for soft tissue density simulation.[2] All samples, including those in the control group, were randomly numbered by the periodontist during the process of recording the presence or absence and (if present) the type of the defect for each block number.

Radiographic examinations

The samples were kept frozen in the intervals between the radiographic examinations in order to prevent moisture loss. Each bone block underwent 3 radiographic examinations: PPA, OPA, and CBCT. A piece of plastic foam with a central slit was designed to incorporate the bone blocks in order to maintain a fixed position during all radiographic procedures. PPA and OPA radiographs were acquired with an intraoral X-ray device (Minray, Soredex, Tuusula, Finland) at standard exposure settings (70 kV, 7 mA, 0.32 s). A size 2 photostimulable phosphor (PSP) plate (Digora Op-
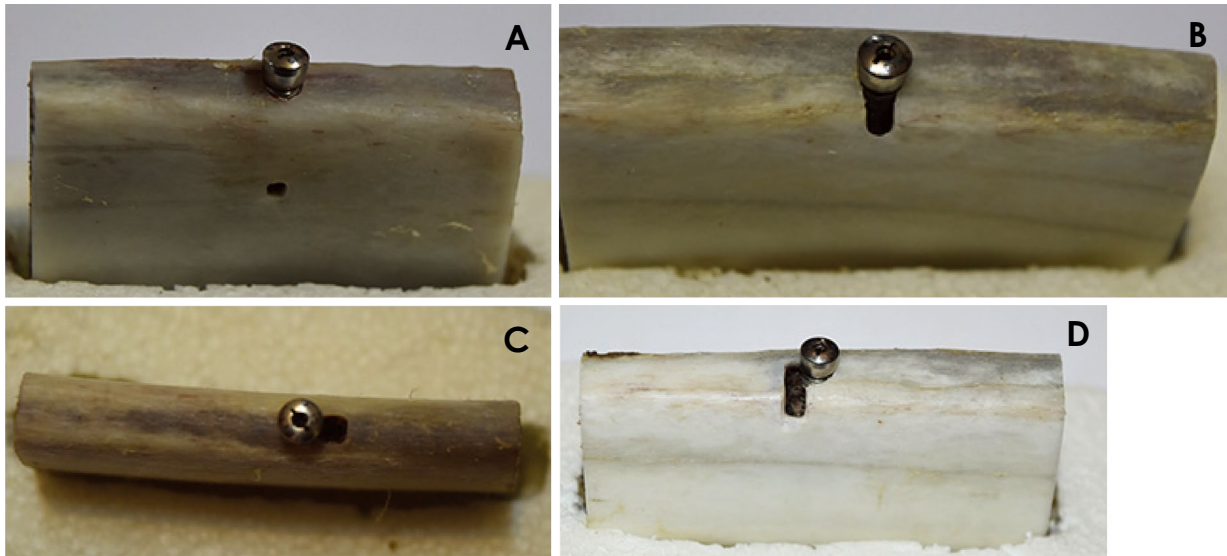
Fig. 1. Peri-implant bone defects created in bovine bone blocks. A. Fenestration defect. B. Dehiscence defect. C. Three-wall defect. D. Two-wall defect.

time, Soredex, Tuusula, Finland) was used. The PSP plate was placed in a holding device that is used with the paralleling technique (Endo-Bite™, Kerr Corporation, Orange, CA, USA). On the top border of the holder's external ring, 2 tongue depressor sticks were attached so that by using a protractor, the first stick was positioned perpendicular to the long axis of the PSP plate and the bone block, while the second was angled 20° mesially (Fig. 2). The horizontal angle of projection was therefore adjusted along the first and second sticks to obtain PPA and OPA radiographs, respectively.

For CBCT examinations, the plastic foam was fixed in the center of the unit's chin rest (Pax-i 3D, Vatech, Yongin, Korea). As in the PPA and OPA examinations, the bone blocks were successively placed inside the central slit of the plastic foam. Images were acquired with a standard protocol of 95 kV, 5.2 mA, a FOV measuring 90×120 mm, and a voxel size of 0.2 mm.

Radiographic assessments

PPA and OPA radiographs were processed and viewed with Scanora imaging software (Version 4.3.1, Digora Optime, Soredex, Tuusula, Finland). CBCT images were exported in the viewer format of the software (Ez3D-i, Vatech, Yongin, Korea). The images were assessed by 2 maxillofacial radiologists. The observers were initially calibrated regarding the radiographic interpretation of peri-implant defects. Both were blinded with regard to the presence and (if present) the type of the bone defect in each sample. The
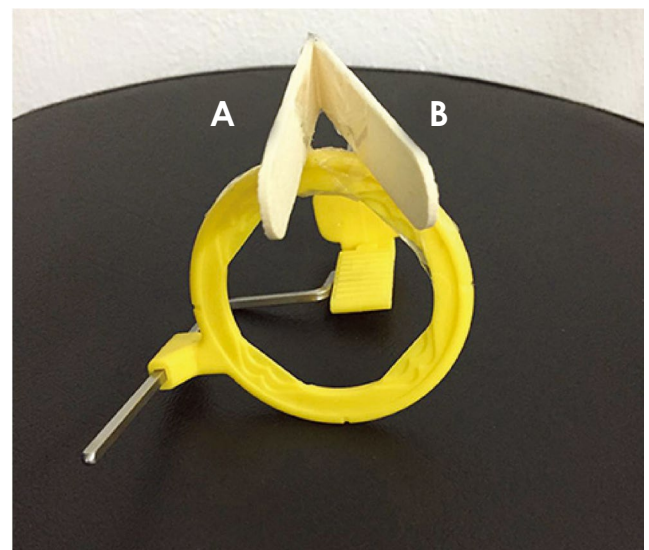

Fig. 2. Tongue depressors attached to the holder device for the acquisition of parallel (A) and oblique (B) periapical radiographs.

image numbers were also randomized in order to minimize the risk of bias. The observers evaluated the images while being allowed to alter the visual parameters, such as brightness and contrast. For the CBCT assessments, the observers could also scroll and view the images along any arbitrary reconstruction plane. Image assessments were performed on a medical liquid-crystal display monitor with a 1920×1200 screen resolution (RadiForce MX241W, EIZO Corporation, Hakusan, Japan), and the computer system used for displaying images to the observers was

Green Magnum Plus (Green Planet Co., Tehran, Iran) with an NVIDIA GeForce 210 video graphics card (Nvidia Corporation, Santa Clara, USA). Each observer evaluated the entire set of images twice, separated by a 2-week interval. For the second observation, both the image numbers and their order of presentation were altered. The observers were provided with a checklist to define the presence or absence as well as (if present) the type of the bone defect for each sample.

Statistical analysis

All data were imported into SPSS software version 16 (SPSS Inc., Chicago, IL, USA). Cohen's kappa (κ) was calculated to evaluate the interobserver reliability. Comparison of the results obtained from the 3 radiographic techniques was performed using the Fisher exact and chi-square tests. A P value less than 0.05 was considered to indicate statistical significance. The area under the receiver operating characteristic curve (AUC), sensitivity, and specificity of each technique were calculated using the Delong method with MedCalc software (version 18.9.1, MedCalc Inc., Ostend, Belgium).

Results

The results of the first and second observations were completely consistent for each examiner. The interobserver agreement was high for assessing both the presence and type of the bone defects ($\kappa = 0.8$-0.9 for PPA and OPA radiography; $\kappa = 1$ for CBCT), and the differences between these values were not statistically significant ($P < 0.001$).

The presence and type of all of the defects were correctly diagnosed using CBCT, and this technique demonstrated the highest values for AUC, sensitivity, and specificity of the methods used. Angular defects were detected with similarly high sensitivity by all 3 radiographic modalities. The

Table 1. Detection of the presence of bone defects by the 3 radiographic techniques

		Angular	Fenestration	Dehiscence
Parallel periapical radiography	AUC	0.95	0.65	0.50
	95% CI	0.751-0.999	0.408-0.846	0.272-0.728
	Sensitivity (%)	100	40	10
	Specificity (%)	90	90	90
Oblique periapical radiography	AUC	0.95	0.95	0.65
	95% CI	0.751-0.999	0.751-0.999	0.408-0.846
	Sensitivity (%)	100	100	40
	Specificity (%)	90	90	90
Cone-beam computed tomography	AUC	1	1	1
	95% CI	0.832-1	0.832-1	0.832-1
	Sensitivity (%)	100	100	100
	Specificity (%)	100	100	100

AUC: area under the receiver operating characteristic curve

Table 2. Detection of the type of bone defects by the 3 radiographic techniques

		Angular	Fenestration	Dehiscence
Parallel periapical radiography	AUC	0.90	0.60	0.50
	95% CI	0.683-0.988	0.361-0.809	0.272-0.728
	Sensitivity (%)	90	30	10
	Specificity (%)	90	90	90
Oblique periapical radiography	AUC	0.85	0.95	0.65
	95% CI	0.621-0.968	0.751-0.999	0.408-0.846
	Sensitivity (%)	80	100	40
	Specificity (%)	90	90	90
Cone-beam computed tomography	AUC	1	1	1
	95% CI	0.832-1	0.832-1	0.832-1
	Sensitivity (%)	100	100	100
	Specificity (%)	100	100	100

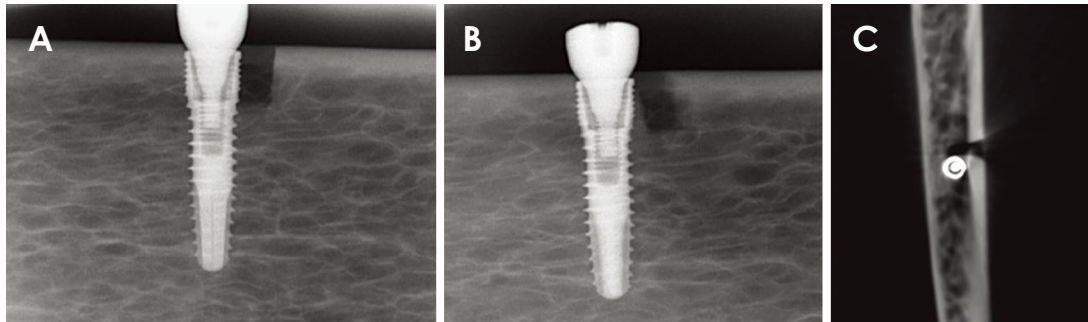AUC: area under the receiver operating characteristic curve

Fig. 3. Radiographic images of a 2-wall angular defect. A. Parallel periapical radiograph. B. Oblique periapical radiograph. C. Axial cone-beam computed tomographic image.
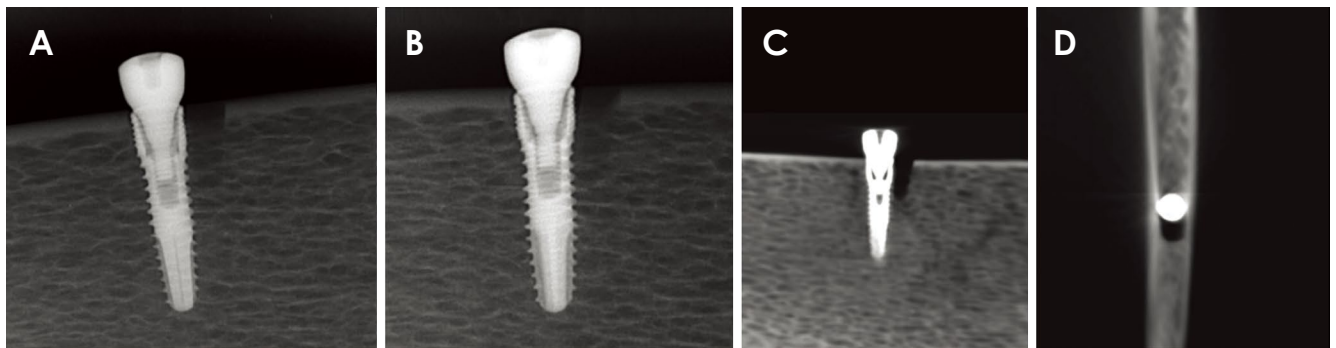

Fig. 4. Radiographic images of a 3-wall angular defect. A. Parallel periapical radiograph. B. Oblique periapical radiograph. C. Tangential cone-beam computed tomographic image. D. Axial cone-beam computed tomographic image.

Table 3. Comparison of the radiographic techniques for detecting the type of angular defects

Radiographic technique	Type detection		Fisher exact test
	Correct diagnoses, N (%)	Incorrect diagnoses, N (%)	
Parallel periapical radiography	9 (90)	1 (10)	
Oblique periapical radiography	8 (80)	2 (20)	$P>0.05$
Cone-beam computed tomography	10 (100)	0 (0)	

AUC and sensitivity of CBCT and OPA were quite similar for the detection of the fenestration defects. CBCT had the highest sensitivity for diagnosis of the dehiscence defects, followed by OPA and PPA, respectively. The specificity of the 3 radiographic techniques was high for all defect types, suggesting that negative diagnoses made on the basis of radiography may be reliable overall. Tables 1 and 2 present the AUC, sensitivity, and specificity values of each radiographic technique.

The presence of all of the 2- and 3-wall angular defects was diagnosed correctly with the 3 radiographic methods (Figs. 3 and 4). The detection of the type of these defects was best accomplished by CBCT, followed by PPA and OPA, respectively (Table 3). The diagnoses of the fenestra-tion and dehiscence defects differed significantly among the imaging techniques (Tables 4 and 5), with PPA being the least efficient (Figs. 5 and 6). No significant difference existed among CBCT, PPA, and OPA with regard to diagnosis of the control group ($P=0.999$).

Discussion

Improper biomechanical features and plaque-induced inflammation are the 2 main etiological factors in the formation of peri-implant bone defects, which can eventually lead to progressive peri-implant bone loss and loss of the implant itself if undetected.[14-16] Therefore, early diagnosis of bone defects is of great importance for preservation of

Table 4. Comparison of the radiographic techniques for detecting the presence and type of fenestration defects

Radiographic technique	Presence detection		Type detection		Fisher exact test
	True, N (%)	False, N (%)	True, N (%)	False, N (%)	
Parallel periapical radiography	4 (40)	6 (60)	3 (30)	7 (70)	
Oblique periapical radiography	10 (10)	0 (0)	10 (10)	0 (0)	$P<0.05$
Cone-beam computed tomography	10 (10)	0 (0)	10 (10)	0 (0)	

True: correct diagnoses, False: incorrect diagnoses

Table 5. Comparison of the radiographic techniques for detecting the presence and type of dehiscence defects

Radiographic technique	Presence detection		Type detection		Chi-square test
	True, N (%)	False, N (%)	True, N (%)	False, N (%)	
Parallel periapical radiography	1 (10)	9 (90)	1 (10)	9 (90)	
Oblique periapical radiography	4 (40)	6 (60)	4 (40)	6 (60)	$P<0.05$
Cone-beam computed tomography	10 (10)	0 (0)	10 (10)	0 (0)	

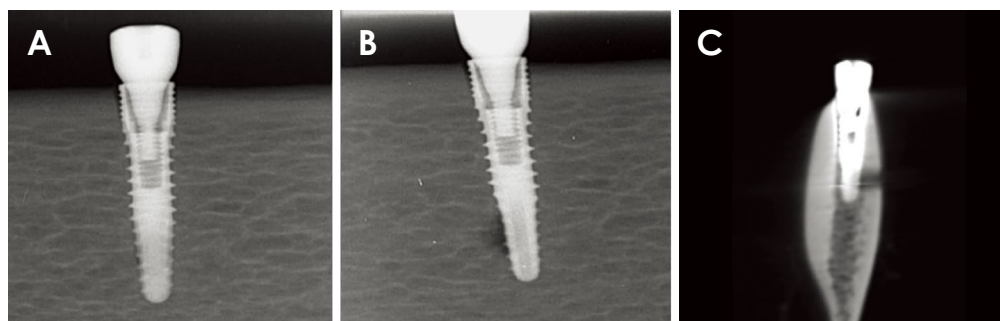True: correct diagnoses, False: incorrect diagnoses

Fig. 5. Radiographic images of a fenestration defect. A. Parallel periapical radiograph. B. Oblique periapical radiograph. C. Cross-sectional cone-beam computed tomographic image.
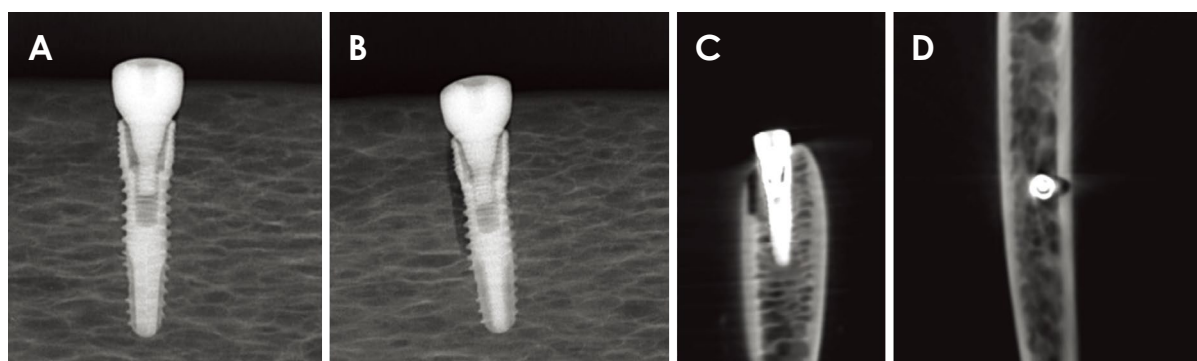

Fig. 6. Radiographic images of a dehiscence defect. A. Parallel periapical radiograph. B. Oblique periapical radiograph. C. Cross-sectional cone-beam computed tomographic image. D. Axial cone-beam computed tomographic image.

the implants and their surrounding bone structure, rendering radiographic assessments necessary.

The position, configuration, and size of a defect greatly influence its visibility on radiographs.[17,18] Silveiro-Ne-to et al.[16] reported that peri-implant defects on the buccal aspect of dental implants were not identifiable on PPA radiographs, while proximal defects were readily diagnosed. Dave et al.[3] assessed the radiographic visibility of peri-im-

plant defects of varying sizes. They found that defects as small as 0.35 mm were only detected on periapical radiographs; larger defects, however, were identified by CBCT as well.

In the present study, 3 relatively common types of peri-implant bone defects with different configurations and positions were evaluated. Preparation of the bone defects was performed in a standard fashion derived from the study conducted by Mengel et al.[19] Angular defects were created, half as 2-wall and half as 3-wall defects. Fenestrations and dehiscences were prepared on the buccal aspect of the implants. In all defect types, none of the dimensions exceeded 3 mm, as this is the critical threshold considered by previous studies with regard to whether a defect is large or small.[6] The clinical relevance of our selection of various defect types was underscored by the fact that defect configuration directly affects treatment outcome.[20]

CBCT, PPA, and OPA were the 3 radiographic techniques assessed. As far as the authors are aware, this is the first study to evaluate periapical radiographs taken obliquely for visualization of peri-implant bone defects and to compare the results with those obtained with PPA and CBCT. The benefits of CBCT include images that are free of distortion and superimposition; however, relatively high radiation exposure and streaking artifacts in the vicinity of metallic objects have limited the application of this technique as a routine follow-up method for dental implants.[6] In contrast, periapical radiographs obtained with the paralleling technique are routinely used for the postoperative evaluation of implants due to their high spatial resolution and negligible radiation dose administered.[21]

Hilgenfeld et al.,[6] Sirin et al.,[20] and Kuhl et al.[21] reported high sensitivity in the detection of various peri-implant defects using CBCT. Furthermore, Dave et al.,[3] Bagis et al.,[4] and Mengel et al.[19] reported that periapical radiographs failed to reveal fenestration and dehiscence defects on the facial aspect of implants. Likewise, in a study performed by Eskandarloo et al.,[22] periapical radiographs and 3 CBCT systems were compared regarding the detection of peri-implant fenestrations. Periapical radiographs were found to be incapable of revealing the defects. This is best explained by these studies' use of the paralleling technique to acquire the periapical radiographs.

In the present study, the highest sensitivity and specificity in the diagnosis of various defect types were observed with the use of CBCT. This appears to be due to the ability to assess the peri-implant bone in any desired orthogonal and non-orthogonal direction, which outweighed the adverse effects of streaking artifacts adjacent to the implants.

A high level of interexaminer reliability with no significant differences was observed for all the radiographic techniques. The presence of all of the angular defects was diagnosed correctly in both the PPA and OPA techniques. The type of these defects, however, was best diagnosed by CBCT imaging and most poorly distinguished by OPA radiographs, although the differences were not statistically significant ($P = 0.754$). The diagnosis of the presence and type of the fenestration and dehiscence defects differed significantly among the 3 radiographic methods ($P < 0.05$). Interestingly, the presence and type of all of the fenestrations were properly diagnosed with the use of OPA radiographs. This is a remarkable finding, as it suggests that the accuracy of OPA is comparable to that of CBCT for the detection of fenestrations. Dehiscences, in contrast, were diagnosed less precisely than fenestrations when using OPA radiographs. This might be attributed to the more longitudinal configuration of these defects, which renders their detection difficult on PA views even when obliquely projected. However, OPA was still more effective than PPA in the detection of dehiscence defects.

There were also limitations to this *in vitro* study that could be further investigated in future clinical experiments. First, peri-implant bone defects may take on relatively bizarre shapes in a clinical context compared to the standard forms used in the present study. Moreover, since soft tissue inflammation concomitantly occurs with peri-implant defects, the impact of such inflammation on the radiographic appearance of these defects must be evaluated.

In conclusion, the sensitivity of CBCT, PPA, and OPA was similarly high for the detection of angular defects. However, fenestration and dehiscence defects were poorly diagnosed by PPA radiographs, while CBCT and OPA were capable of revealing these defects. The addition of OPA radiographs to routine PPA imaging would be remarkably beneficial as a radiographic follow-up method for patients with dental implants, particularly when a reasonable suspicion exists of bone defects in the bucco-lingual aspect. Although accurate in detecting all of the defect types, CBCT during follow-up should be selectively applied in cases that satisfy certain indications due to the greater amount of radiation administered and the higher cost of this technique.

Conflicts of Interest: None

References

1. Ding Q, Zhang L, Geraets W, Wu W, Zhou Y, Wismeijer D,

et al. Association between peri-implant bone morphology and marginal bone loss: a retrospective study on implant-supported mandibular overdentures. Int J Oral Maxillofac Implants 2017; 32: 147-55.

2. Kamburoğlu K, Murat S, Kılıç C, Yüksel S, Avsever H, Farman A, et al. Accuracy of CBCT images in the assessment of buccal marginal alveolar peri-implant defects: effect of field of view. Dentomaxillofac Radiol 2014; 43: 20130332.

3. Dave M, Davies J, Wilson R, Palmer R. A comparison of cone beam computed tomography and conventional periapical radiography at detecting peri-implant bone defects. Clin Oral Implants Res 2012; 24: 671-8.

4. Bagis N, Kolsuz ME, Kursun S, Orhan K. Comparison of intraoral radiography and cone-beam computed tomography for the detection of periodontal defects: an in vitro study. BMC Oral Health 2015; 15: 64.

5. Bohner LO, Mukai E, Oderich E, Porporatti AL, Pacheco-Pereira C, Tortamano P, et al. Comparative analysis of imaging techniques for diagnostic accuracy of peri-implant bone defects: a meta-analysis. Oral Surg Oral Med Oral Pathol Oral Radiol 2017; 124: 432-40.e5.

6. Hilgenfeld T, Juerchott A, Deisenhofer UK, Krisam J, Rammelsberg P, Heiland S, et al. Accuracy of cone-beam computed tomography, dental magnetic resonance imaging, and intraoral radiography for detecting peri-implant bone defects at single zirconia implants - an in vitro study. Clin Oral Implants Res 2018; 29: 922-30.

7. Saberi BV, Khosravifard N, Mohtavipour T, Khaksari F, Abbasi S, Shahmalakpoor A. Entrance skin dose of the thyroid gland area following exposure with different protocols of two panoramic and cone-beam computed tomography devices. J Oral Maxillofac Radiol 2019; 7: 6-11.

8. Khojastepour L, Haghnegahdar A, Khosravifard N. Role of sinonasal anatomic variations in the development of maxillary sinusitis: a cone beam CT analysis. Open Dent J 2017; 11: 367-74.

9. de-Azevedo-Vaz SL, Peyneau PD, Ramirez-Sotelo LR, Vasconcelos Kde F, Campos PS, Haiter-Neto F. Efficacy of a cone beam computed tomography metal artifact reduction algorithm for the detection of peri-implant fenestrations and dehiscences. Oral Surg Oral Med Oral Pathol Oral Radiol 2016; 121: 550-6.

10. de-Azevedo-Vaz SL, Vasconcelos Kde F, Neves FS, Melo SL, Campos PS, Haiter-Neto F. Detection of periimplant fenestration and dehiscence with the use of two scan modes and the smallest voxel sizes of a cone-beam computed tomography device. Oral Surg Oral Med Oral Pathol Oral Radiol 2013; 115: 121-7.

11. Liedke GS, Spin-Neto R, da Silveira HE, Schropp L, Stavropoulos A, Wenzel A. Factors affecting the possibility to detect buccal bone condition around dental implants using cone beam computed tomography. Clin Oral Implants Res 2017; 28: 1082-8.

12. Mikolajczak T, Wilk G. The diagnostic value of oblique technique for periapical radiography and its usefulness in endodontic treatment. Ann Acad Med Stetin 2008; 54: 94-8.

13. Pinheiro LR, Scarfe WC, Augusto de Oliveira Sales M, Gaia BF, Cortes AR, Cavalcanti MG. Effect of cone-beam computed tomography field of view and acquisition frame on the detection of chemically simulated peri-implant bone loss in vitro. J Periodontol 2015; 86: 1159-65.

14. Salvi GE, Cosgarea R, Sculean A. Prevalence and mechanisms of peri-implant diseases. J Dent Res 2017; 96: 31-7.

15. Khoshkam V, Chan HL, Lin GH, MacEachern MP, Monje A, Suarez F, et al. Reconstructive procedures for treating peri-implantitis: a systematic review. J Dent Res 2013; 92 (12 Suppl): 131s-8s.

16. Silveira-Neto N, Flores ME, De Carli JP, Costa MD, Matos FS, Paranhos LR, et al. Peri-implant assessment via cone beam computed tomography and digital periapical radiography: an ex vivo study. Clinics (Sao Paulo) 2017; 72: 708-13.

17. Ritter L, Elger MC, Rothamel D, Fienitz T, Zinser M, Schwarz F, et al. Accuracy of peri-implant bone evaluation using cone beam CT, digital intra-oral radiographs and histology. Dentomaxillofac Radiol 2014; 43: 20130088.

18. Schwarz F, Sahm N, Schwarz K, Becker J. Impact of defect configuration on the clinical outcome following surgical regenerative therapy of peri-impantitis. J Clin Periodontol 2010; 37: 449-55.

19. Mengel R, Kruse B, Flores-de-Jacoby L. Digital volume tomography in the diagnosis of peri-implant defects: an in vitro study on native pig mandibles. J Periodontol 2006; 77: 1234-41.

20. Sirin Y, Horasan S, Yaman D, Basegmez C, Tanyel C, Aral A, et al. Detection of crestal radiolucencies around dental implants: an in vitro experimental study. J Oral Maxillofac Surg 2012; 70: 1540-50.

21. Kühl S, Zürcher S, Zitzmann NU, Filippi A, Payer M, Dagassan-Berndt D. Detection of peri-implant bone defects with different radiographic techniques - a human cadaver study. Clin Oral Implants Res 2016; 27: 529-34.

22. Eskandarloo A, Saati S, Ardakani MP, Jamalpour M, Gholi Mezerji NM, Akheshteh V. Diagnostic accuracy of three cone beam computed tomography systems and periapical radiography for detection of fenestration around dental implants. Contemp Clin Dent 2018; 9: 367-81.